Inorg. Chem. **2005**, *44*, 6393–6400

Fabrication of ZnSe Nanoparticles in the Apoferritin Cavity by Designing a Slow Chemical Reaction System

Kenji Iwahori,[†,‡] Keiko Yoshizawa,[†] Masahiro Muraoka,[†] and Ichiro Yamashita*[,†,‡]

CREST, Japan Science and Technology Agency, 4-1-8 Honcho, Kawaguchi, Saitama, Japan, and Advanced Technology Research Laboratories, Matsushita Electronic Industrial Company, Ltd., 3-4 Hikaridai, Seika, Kyoto, Japan

Received February 16, 2005

Zinc selenide nanoparticles (ZnSe NPs) were synthesized in the cavity of the cage-shaped protein apoferritin by designing a slow chemical reaction system, which employs tetraaminezinc ion and selenourea. The chemical synthesis of ZnSe NPs was realized in a spatially selective manner from an aqueous solution, and ZnSe cores were formed in almost all apoferritin cavities with little bulk precipitation. Three factors are found to be important for ZnSe NP synthesis in the apoferritin cavity: (1) the threefold channel, which selectively introduces zinc ion into the apoferritin cavity, (2) the apoferritin internal potential, which favors zinc ion accumulation in the cavity, and (3) the nucleation site, which nucleates ZnSe inside the cavity. The characterization of the synthesized ZnSe NPs by X-ray powder diffraction and energy-dispersive spectrometry revealed that the synthesized NPs are a collection of cubic ZnSe polycrystals. It was shown that the 500 °C heat treatment for 1 h under nitrogen gas transformed the polycrystalline ZnSe core into a single crystal, and single-crystal ZnSe NPs free of protein were obtained.

1. Introduction

Nanoparticles (NPs) have recently attracted great interest because of their potential to be used as components in nanotechnology. Magnetic NPs make it possible to produce high-density storage memory media. Some metal NPs have much higher catalytic activity than a bulk metal surface. Furthermore, conductive or semiconductor NPs are small enough for the electron energy level to be quantized and are expected to be used as quantum dots. Therefore, many methods to produce NPs have been studied. Physical methods include grinding materials, laser abrasion, and ion injection. Chemical methods include the sol−gel method and the TOPO method.[1] Using a nanometric cavity for synthesizing NP is another method that has been developed.

There are papers reporting the production of inorganic NPs in the cavity of the cage-shaped protein apoferritin, a major cellular iron-storage protein.[2−10] Recently, Ag NPs have been produced in the chimerical apoferritin with the silver nucleating peptide.[11] The native apoferritin consists of 24 polypeptide subunits. There are two types of subunits, the light-chain subunit (L subunit) and the heavy-chain subunit (H subunit), and the ferroxidase center in an H subunit oxidizes ferrous iron to ferric iron. The inner and outer diameters of the protein shell are about 7 and 12 nm, respectively. The cavity and outside bulk solution are connected with narrow channels. This inner cavity stores about 4000 iron atoms as the mineral ferrihydrite *in vivo*. The electrostatic gradient near the surface of recombinant ferritin was calculated utilizing the Poisson−Boltzmann equation. The electrostatic potential calculations to study the functional roles of the threefold and fourfold channels also have been performed.[12,13] These preceding works indicated

* To whom correspondence should be addressed. E-mail: ichiro@ms.naist.jp. Present address: Nara Institute of Science and Technology, 8916-5 Takayama, Ikoma, Nara 630-0101, Japan. Tel: +81-743-72-6196. Fax: +81-743-72-6196.

† CREST, Japan Science and Technology Agency.

‡ Matsushita Electronic Industrial Co.

(1) Murray, V. B.; Norris, D. J.; Bawendi, M. G. *J. Am. Chem. Soc.* **1993**, *115*, 8706.
(2) Meldrum, F. C.; Wade, V. J.; Nimmo, D. L.; Heywood, B. R.; Mann, S. *Nature* **1991**, *349*, 684.
(3) Meldrum, F. C.; Heywood, B. R.; Mann, S. *Science* **1992**, *257*, 552.
(4) Mann, S. *Nature* **1993**, *365*, 499.
(5) Douglas, T.; Dickson, D. P. E.; Betteridge, S.; Charnock, J.; Garner, C. D.; Mann, S. *Science* **1995**, *269*, 54.
(6) Meldrum, F. C.; Douglas, T.; Levi, S.; Arosio, P.; Mann, S. *J. Inorg. Biochem.* **1995**, *58*, 59.
(7) Douglas, T.; Stark, V. T. *Inorg. Chem.* **2000**, *39*, 1828.
(8) Okuda, M.; Iwahori, K.; Yamashita, I.; Yoshimura, H. *Biotechnol. Bioeng.* **2003**, *84*, 187.
(9) Wong, K. K. W.; Mann, S. *Adv. Mater.* **1996**, *8*, 928.
(10) Ueno, T.; Suzuki, M.; Goto, T.; Matsumoto, T.; Nagayama, K.; Watanabe, Y. *Angew. Chem., Int. Ed.* **2004**, *43*, 2527.
(11) Kramer, M. R.; Li, C.; Carter, C. D.; Stone, O. M.; Naik, R. R. *J. Am. Chem. Soc.* **2004**, *126*, 13282.

10.1021/ic0502426 CCC: $30.25
Published on Web 08/04/2005

that the electrostatic potential profile enhanced positive iron ion introduction into the apoferritin cavity. The threefold channel is shown to be responsible for the transit positive iron ions. Using apoferritin as a spatially restricted chemical reaction chamber in aqueous conditions, the inorganic NPs were synthesized in the apoferritin cavity by selecting the appropriate buffer conditions *in vitro*. The obtained NPs have a narrow size distribution because the apoferritin molecules all have the same size.

Reports of the inorganic NPs synthesized within apoferritin have so far been mostly metal complex NPs. It is of great interest to synthesize semiconductor NPs within the apoferritin cavity. There are only two reports describing semiconductor NP synthesis in the cage-shaped protein. Small cadmium sulfide (CdS) cores with 275 Cd and S atoms were formed in the apoferritn cavity,[9] and homogeneous cadmium selenide (CdSe) semiconductor NPs were recently synthesized.[14] CdSe semiconductor NPs were almost fully developed in the apoferritin cavity, the average diameter was 7 nm, which is the same as that of apoferritin cavity, and the dispersion of diameters was small. Because the electron energy levels of the semiconductor NPs are quantized depending on their size and shape, this is an ideal characteristic for a nanoelectronics device component, i.e., a quantum dot. Namely, CdSe NPs synthesized by the biological path are very attractive from the nanoelectronics point of view. However, Cd ions can easily bind to the Cd-binding site near the twofold axis of the ferritin molecule and form the huge bulk precipitation of apoferritin complexes. This phenomenon hinders the optimization of CdSe NPs synthesized in apoferritin and the analysis of the biomineralization mechanism.

In this paper, we report the successful synthesis of homogeneous zinc selenide (ZnSe) NPs in the apoferritin cavity. ZnSe is a promising material for n-type semiconductors. ZnSe NPs emit fluorescent light and could be used as quantum labels for biological use because the fluorescent light does not quench. We have already designed a new chemical process that achieves the nucleation and full development of semiconductor NPs in the apoferritin cavity. The optimization of this chemical reaction system for ZnSe and the structure analysis of the obtained ZnSe NPs by X-ray powder diffraction (XRD) and energy-dispersive spectrometry (EDS) measurement are described. The possible biomineralization mechanism is also discussed, which will give a valuable base for the synthesis of a variety of compound semiconductor NPs in the apoferritin cavity.

2. Experimental Section

2.1. ZnSe Introduction into the Apoferritin Cavity. The horse spleen apoferritin (HsAFr) was purchased from Sigma. All chemicals were purchased from Sigma-Aldrich and used as received with no further purification.

The reaction solution for synthesized ZnSe NPs in the apoferritin cavity includes the zinc ion, serenium ion, ammonium ion, and 0.3 mg/mL, i.e., 0.66 μM HsAFr. The pH of the reaction solution was adjusted by adding ammonia water. One apoferritin cavity theoretically accommodates about 1000 ZnSe atoms as a ZnSe crystal. Therefore, 0.66 mM zinc ion concentration is enough to fill the apoferritin cavity. The zinc ion concentration was fixed slightly in excess, i.e., 1 mM, for safety. Because selenium ions were supplied by selenourea slowly, the selenium ion concentration was fixed at 5 mM to supply enough selenium ions. The concentration of the ammonium ion should be high enough to coordinate the zinc ion and make the tetraaminezinc ion stable. Therefore, the ammonium ion concentration was fixed at 40 mM, which is 10 times more than the concentration necessary to coordinate all zinc ions.

When the pH dependence on the ZnSe NPs synthesis in the apoferritins is surveyed, a 5-mL reaction mixture solution with a final concentration of 0.3 mg/mL HsAFr, 1 mM zinc acetate, 40 mM ammonium acetate, and 5 mM selenourea was prepared, and the pH of the mixture solution was adjusted by adding ammonia water up to 15 mM. When the dependence of buffer reagents on ZnSe NP formation is studied, five buffer reagents, Tris-HCl, sodium phosphate, TAPS, HEPES, and KH_2PO_4−NaOH buffers, were used to maintain the solution at pH 8.0. In the case of optimization of the selenium ion concentration, a 5-mL reaction mixture solution with a final concentration of 0.3 mg/mL HsAFr, 1 mM zinc acetate, 40 mM ammonium acetate, and 7.5 mM ammonia water was prepared, and selenourea was added with a final concentration of up to 15 mM. In the case of optimization of the zinc ion concentration, a 5-mL reaction mixture solution with a final concentration of 0.3 mg/mL HsAFr, 40 mM ammonium acetate, 7.5 mM ammonia water, and 10 mM selenourea was prepared, and zinc acetate was added with a final concentration of up to 5 mM.

In every experiment, the addition of selenourea was the final step, except in the case when zinc was added last. Selenourea (100 mM or 1 M) was dissolved in pure water with a minimal amount of ethanol just before use and added to the reaction mixture solution. The solution was left overnight at room temperature to ensure that the reaction goes to completion. The synthesis of ZnSe could be monitored by the color change of the reaction mixture solution. That color was transparent at the beginning and changed to light reddish pink after several hours because of the synthesis of ZnSe. Usually, we dialyze and concentrate synthesized ZnSe NPs to remove any amount of material from the apoferritin. After that treatment, the concentrated ZnSe−ferritin solution is applied to the SW4000 XL (Tosoh Co., Tokyo, Japan) gel filtration column to remove the impurities as necessary.

2.2. Iron Ion Introduction into the Apoferritin Cavity. The 5-mL reaction mixture including the final concentration of the 0.3 mg/mL HsAFr or recombinant apoferritins and 150 mM NaCl was adjusted at pH 7.0 by 100 mM HEPES. Also, 3 mM ammonium ferrous sulfate was added to the reaction mixture last. This reaction was performed at room temperature.

2.3. Transmission Electron Microscopy (TEM) Observation. After synthesis of NPs in the apoferritin cavity, the reaction mixture solutions were centrifuged at low speed and the supernatant was carefully retrieved to remove any bulk precipitate and aggregation products. Several microliters of the supernatant were put on the carbon film coated mesh for TEM, and excessive solution was removed. The samples were negatively stained by 1% aurothioglucose and observed by TEM (JEOL 1010 and Topcon EM-002B). The core formation ratio (CFR) was calculated by dividing the number of core-containing apoferritins by the number of all apoferritins in TEM images and used for the evaluation of core formation efficiency.

(12) Douglas, T.; Ripoll, R. D. *Protein Sci*. **1998**, *7*, 1083.
(13) Takahashi, T.; Kuyucak, S. *Biophys. J*. **2003**, *84*, 2256.
(14) Yamashita, I.; Hayashi, J.; Hara, M. *Chem. Lett*. **2004**, *33*, 1158.

2.4. XRD Measurement. A total of 50 mg of purified HsAFr with ZnSe cores was treated with a pH 12 solution, and the ZnSe NPs were collected with low-speed centrifugation. The ZnSe pellet was intensively washed with pure water by several cycles of suspension and centrifugation. The pellet was then nitrogen gas dried and was gently ground using a mortar. A part of the fine powder obtained was placed in a quartz tube of 3 cm diameter and heat-treated for 1 h under nitrogen gas with a 100 mL/min flow rate at 500 °C. The X-ray generator (RINT2500/PC; Rigaku Corp., Tokyo, Japan) was operated at 50 kV and 200 mA with a Cu target, and XRD measurements were carried out before and after heat treatment.

2.5. Construction and Purification of Recombinant L-Chain Apoferritins. We previously made the Fer0 mutant with the plasmid pKIT0 coded from the full length amino acids (1−175) of L-chain apoferritin from horse liver.[11] We also make the deletion mutant Fer8, which includes 9−175 amino acids of L-chain apoferritin, because commercially available natural apoferritin also lacks the first eight amino acids of L-chain apoferritin.[15] The mutant Fer8 was constructed by cloning an L-chain apoferritin DNA fragment-deleted 24 bp of the 5′ end from PCR product in EcoRI-HindIII-digested pMK2.[8] We named this plasmid pKIT8. pKIT8 transformed into NovaBlue competent cells (Novagen), and the resultant Fer8 mutant produced the modified L-chain apoferritin, which consisted of residues 9−175 amino acids.

The 8A recombinant apoferritin, Asp131Ala/Glu134Ala, and the 8AK recombinant apoferritins, Asp131Ala/Glu134Ala and Glu58Lys/Glu61Lys/Glu64Lys, were constructed by the PCR-based mutagenesis techinique.[16,17] Supercoiled pKIT8 plasmid DNA was used as a template in PCRs carried out with antiparallel pairs of primer, which contained the desired point mutations. The PCR products by pfu-Turbo DNA polymerase (Stratagene) were treated with DpnI, which exclusively degraded methylated template DNA. The resulting DNAs (pKIT8A and pKIT8AK) were ligated and transformed into *Escherichia coli*. Mutations were verified by DNA sequence analysis. Resultant 8A and 8AK mutants produced the modified L-chain apoferritins, 8A recombinant apoferritin and 8AK recombinant apoferritin.

All of the mutants (Fer8, 8A, and 8AK) were cultured in 3 L of an LB medium including ampicillin (100 μg/mL) at 37 °C for 16 h. After cultivation, mutant cells were harvested by centrifugation and resuspended in 15 mL of a 50 mM Tris-HCl buffer (pH 8.0). Then, the suspension was disrupted by ultrasonic oscillation (Sonifer 250; Branson Ultrasonic Corp., Danbury, CT) in an ice bath for 2 min and repeated three or four times. Cell debris was removed by centrifugation at 12 000 rpm for 20 min, and the supernatant were treated at 65 °C for 20 min to denature impurities except recombinant apoferritin. The supernatant obtained after centrifugation was applied to a Q-sepharose HP column (∅ 2.0 × ∼10 cm; Amersham Biosciences, Buckinghamshire, U.K.) equilibrated with a 50 mM Tris-HCl buffer (pH 8.0). The recombinant apoferritin was eluted using a 50 mM Tris-HCl buffer with a linear NaCl gradient from 100 to 500 mM. Each fraction containing recombinant apoferritin was collected. The solution was concentrated to 2−3 mL and applied to a Sephacryl S-300 (∅ 2.6 × ∼60 cm; Amersham Biosciences, Buckinghamshire, U.K.) gel filtration column chromatograph equilibrated with a 50 mM Tris-HCl buffer with 150 mM NaCl (pH 8.0). To check the purity of monomeric 24-subunit recombinant apoferritin, each eluted fraction from the Sepahcryl S-300 column was analyzed by a SW4000 XL (Tosoh Co., Tokyo, Japan) gel filtration column chromatograph. The monomeric recombinant apoferritin fractions after a Sepahcryl S-300 column were collected and used as the purified apoferritin in the experiment described.

2.6. ICP-MASS Analysis for the Zinc Ion Concentration in the Apoferritin Cavity. We measured the zinc concentration in the zinc^{2+}−apoferritin precursor by the ICP-MASS. The zinc^{2+}−apoferritin precursor was prepared under optimum conditions without 10 mM selenourea addition by the method described in section 2.1. The purified zinc^{2+}−apoferritins were washed four times and dialyzed overnight against deionized water. Then, zinc^{2+}−apoferritins were resolved in nitric acid and analyzed by the ICP-MASS (HP4500; Yokokawa, Japan).

3. Results and Discussion

3.1. Design of a New Chemical Reaction System for ZnSe Core Formation. Our preliminary experiment of mixing 1 mM zinc acetate and 5 mM selenic or serenious acid in an aqueous solution showed fast aggregation of ZnSe, even when 0.3 mg/mL apoferritins were present in the solution. From many mineralization reactions, apoferritin has the ability to suppress bulk precipitation, but in the case of zinc and selenium ions, the chemical reaction is too intense to be suppressed. As a result, apoferritin molecules coprecipitated with ZnSe aggregates, and there were a few molecules in the supernatant of the reaction mixture. Furthermore, the remaining apoferritins in the supernatant did not accommodate ZnSe cores. This is because zinc and selenium ions react so fast under the aqueous conditions that the ion added last could not reach the apoferritin cavity. They react only in the bulk solution, resulting in ZnSe precipitation. Therefore, we designed a new chemical reaction system, which is composed of a slow chemical reaction and a two-step synthesis protocol.

First, a slow chemical reaction was designed, employing tetraaminezinc ion and selenourea. It is known that zinc ions are stabilized by coordination of ammonia to form positively charged tetraaminezinc ions. Selenourea is unstable in an aqueous solution and slowly degrades, releasing selenium ions into the aqueous solution over several days. When stable tetraaminezinc ion and unstable selenourea are combined, slow ZnSe synthesis should be achieved.

Second, the two-step chemical reagent mixture is designed to initiate faster nucleation inside the apoferritin shell than outside. Because the inner surface of the apoferritin cavity has many acidic amino acid residues, the inner space has a negative electrostatic potential.[12] Zinc ions outside apoferritin mostly exist as tetraaminezinc ions and some hydrated zinc ions in chemical equilibrium. These hydrated zinc ions will be concentrated inside the apoferritin cavity by electrostatic attraction. After incubation of apoferritin and zinc ions, the addition of selenourea to the mixture will release selenium ions and ZnSe will be synthesized inside the cavity. Because the zinc ions outside apoferritin are protected as tetraaminezinc ions, ZnSe nucleation will occur only in the apoferritin cavity. Once the nucleus has formed, the ZnSe crystal surface

(15) Takeda, S.; Ohta, M.; Ebina, S.; Nagayama, K. *Biochim. Biophys. Acta* **1993**, *1174*, 218.
(16) Picard, V.; Ersdal-Badju, E.; Lu, U.; Bock, S. C. *Nucleic Acid Res.* **1994**, *22*, 2587.
(17) Imai, I.; Matsushima, Y.; Sugimura, T.; Terada, M. *Nucleic Acid Res.* **1991**, *19*, 2785.

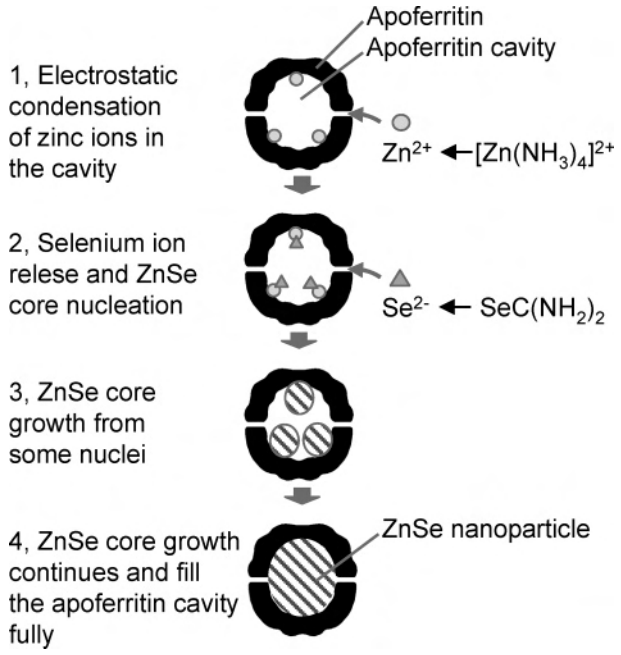

Figure 1. Schematic drawing of the newly designed ZnSe NP synthesis: (1) Electrostatic condensation: Apoferritin molecules are incubated with zinc ions, and zinc ions are condensed in the apoferritin cavity. (2) After incubation, selenium ions are supplied by selenourea, which degrades slowly in an aqueous solution. Because the highly condensed zinc ions react with selenium ions quickly, ZnSe nuclei are produced preferentially in the apoferritin cavity. (3) Once the ZnSe nucleus has been made, the ZnSe NPs grow autocatalytically. (4) ZnSe growth continues until the apoferritin cavity is filled.

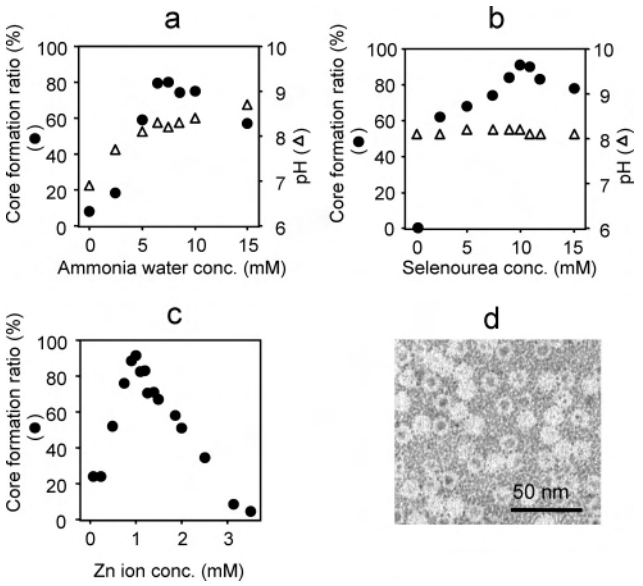

Figure 2. Effects of the concentration of ammonium, selenium, and zinc ions on the ZnSe CFR. (a) The solution pH increases in proportion to the concentration of ammonium ions, and the CFR has a peak around the ammonium concentration of 7.5 mM, which corresponds to pH 8.0−8.2. (b) The CFR has a peak at 10 mM selenourea concentration, and the CFR reached more than 90%. The solution pH is little affected by the addition of selenourea and stays around 8.0−8.2. (c) The CFR has a peak at a zinc ion concentration of 1.0 mM. This is 1.5 times more than the theoretical concentration for fulfillment of all of the apoferritin cavity. (d) TEM image at a zinc ion concentration 0.25 mM, which shows that core formation occurs in an "all-or-nothing" manner.

itself will work as an autocatalyst and ZnSe will be formed quickly in the apoferritin cavity (see Figure 1).

3.2. Verification of the Designed Chemical Reaction System and Optimization of ZnSe NP Synthesis Conditions. We carried out experimental verification of this newly designed slow, two-step ZnSe synthesis method and optimized the reaction conditions, such as the pH of the reaction solution, selenium ion concentration, and zinc concentration.

The solution including 0.3 mg/mL HsAFr, 1 mM zinc ion, 5 mM selenourea, and 40 mM ammonium acetate was freshly prepared, and ammonia water was added up to 15 mM to control the solution pH. After centrifugation (∼3000*g*) to remove precipitation from the reaction mixture, the supernatant was observed by TEM and the pH of the mixture solution was measured. Figure 2a shows the dependence of the ammonia water concentration on the CFR and reaction mixture pH. As the ammonia water increased, the pH monotonically increased from 7.0 to 8.8. The CFR peaked around a 7.5 mM ammonia water concentration, which corresponds roughly to pH 8.2, and the CFR was as high as 80%. In the case of ammonia water concentration higher than 7.5 mM, bulk precipitation was observed. This is because the high pH makes the chemical reaction faster in the bulk solution than the apoferritins are able to take in available zinc and selenium ions. Therefore, zinc and selenium ions left in the solution made bulk precipitation. From this result, the optimum concentration of ammonia water for ZnSe core formation was determined to be 7.5 mM.

Instead of ammonia water, the use of buffer reagents was additionally studied. The same chemical synthesis solutions as those described above were used but were adjusted at pH 8.2 by five kinds of buffer reagents: sodium phosphate buffer, Tris-HCl buffer, TAPS, HEPES, and KH_2PO_4/NaOH buffer. The TEM images revealed that the CFR depends on the kinds of buffer reagents but the CFR never exceeded 45% (data not shown). This may be caused by the interaction between buffer reagents and zinc ions. The buffer agents may coordinate the zinc ion and make a stable zinc ion complex, which cannot go through the threefold channel. Similar results were obtained in the cobalt oxide introduction into the apoferritin cavity.[27] Therefore, it is concluded that buffer reagents should be removed from the slow chemical reaction mixture for ZnSe NP synthesis and the pH was adjusted only by the ammonia water.

Second, the optimum concentration of the selenium ion was surveyed. Because selenourea degrades slowly in an aqueous solution, the supply rate of the selenium ion can be controlled solely by the concentration of selenourea. The higher concentration leads to a faster supply of selenium ions. A reaction mixture solution with a final concentration of 0.3 mg/mL HsAFr, 1 mM zinc acetate, 40 mM ammonium acetate, and 7.5 mM ammonia water was prepared, and selenourea with a final concentration of up to 15 mM was added last. After standing overnight, the supernatant was observed by TEM and the pH of the mixture solution was measured. Figure 2b shows the dependence of the selenourea concentration on the CFR and the pH of the reaction solution. Despite the proton byproducts from the ZnSe synthesis reaction, the excess ammonium acetate buffered the pH change and the pH stayed around 8.2. The CFR showed a

single peak at 10 mM selenourea concentration. This result indicated that there is an optimum supply rate of selenium ions for overnight core formation, which was realized by 10 mM selenourea. In the case of lower concentration, the chemical reaction is slower and takes longer than an overnight period. When the selenium ion was not supplied, no NPs were observed, which indicates that zinc oxide NPs cannot be produced under these solution conditions. In the case of higher concentration, the selenium ion supply is too fast to react with the zinc ions, which come from the tetraaminezinc ion through the chemical equilibrium. The selenium ions, which cannot react with the zinc ions, react themselves and are precipitated as selenium red. This is supported by the experimental result that the structure of this precipitate was determined as selenium by XRD measurement (data not shown).

Third, we studied whether the initial 1 mM zinc ion concentration was appropriate or not because 0.66 mM zinc ion is enough to fill the 0.3 mg/mL HsAFr cavity. The zinc ion from 0.1 to 5 mM was added to the solution (0.3 mg/mL HsAFr, 10 mM selenourea, 7.5 mM ammonium water, and 40 mM ammonium acetate), and the mixed solution was left overnight. The supernatant after centrifugation was observed by TEM, and the pH of the reaction solution was measured. Figure 2c shows the dependence of the zinc ion concentration on the CFR. The CFR increased monotonically until a zinc concentration of 1.0 mM and started decreasing sharply after around 1.0 mM. This optimum point is about 1.5 times more zinc ions than the theoretically calculated capacity of apoferritin. This indicates that a 1.0 mM zinc ion completes the core formation overnight. This is supported by the observation that the solution with 1.0 mM zinc forms the bulk precipitation after longer time periods.

Figure 2d is the TEM image at 0.25 mM zinc ion concentration, which is one-quarter of the optimal zinc ion concentration. The CFR is about 25%, and some apoferritin molecules accommodated fully developed cores while others had no cores. There were no small cores or undeveloped cores in apoferritin cavities. This implies that once the nucleus of ZnSe formed, they grew fast and consumed zinc ion resources quickly, and the resulting low zinc ion concentration increasingly suppresses any further nucleation of ZnSe. As a result, the ZnSe core formation is an "all-or-nothing" type reaction. This is consistent with the preceding literature.[4]

Taking into account all of the above experimental results, the optimum ZnSe core formation condition was determined to be 0.3 mg/mL HsAFr, 1 mM zinc acetate, 40 mM ammonium acetate, 7.5 mM ammonia water, and 10 mM selenourea. Using these optimal conditions, the CFR reached as high as 90%.

Under this optimum condition, it can be estimated how much faster the ZnSe is synthesized in the apoferritin cavity compared to than in the bulk solution. The total apoferritin cavity volume is about 1/20 000 of the bulk solution, and the almost all of the ZnSe NPs were synthesized in the apoferritin cavity. This indicates that the synthesis rate in apoferritin is at least 20 000 times faster than that in the bulk solution. Otherwise, some ZnSe NPs were synthesized in the solution. This may be due to the fast nucleus formation by a highly condensed zinc ion in the apoferritin and autocatalytic ZnSe core formation. The synthesized ZnSe cores in the apoferritin stored at 4 °C is very stable for 3 months at least. We can observe the black dot from ZnSe NPs after 3 months of samples by TEM observation.

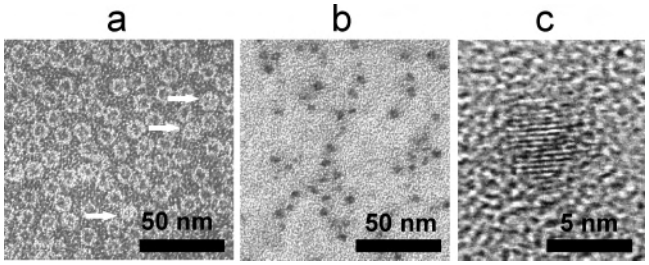

Figure 3. TEM images of ferritin and apoferritin synthesized by the newly designed chemical reaction system. (a) TEM image of the synthesized ZnSe ferritin molecule stained by 1% aurothioglucose. Cores are surrounded by white rings, which are negatively stained protein shells. Almost all molecules accommodate cores except the molecules indicated by arrowheads, which are apoferritin molecules. The CFR was calculated by dividing the number of core-formed apoferritins by all apoferritins in the TEM picture. This typical TEM image of a ZnSe synthesis experiment clearly shows that the CFR is more than 90%. (b) TEM image of the synthesized ZnSe ferritin molecule without stain. The cores are homogeneous. (c) High-magnification core image and the lattice of the ZnSe core crystal clearly observed.

3.3. TEM Observation and Elements Confirmation. The ZnSe NPs synthesized under the optimum conditions were observed by TEM with and without 1% aurothioglucose staining. Typical TEM images are shown in Figure 3. The TEM image negatively stained shows many dots surrounded by ferritin protein shells (Figure 3a). Because aurothioglucose is too big to penetrate through narrow channels, the dots are attributed to the ZnSe cores. The ZnSe−ferritin molecules are well dispersed, and aggregates were not observed. Also ZnSe NPs were not observed outside apoferritin. This corresponds to the fact that the supernatant was clear after overnight core formation.

Figure 3b is a TEM image of ZnSe−ferritins without staining. Because the protein shell is not visualized, only ZnSe NPs are observed. Figure 3c shows the high-magnification image of one core. The clear lattice image was visible, and the core is a single crystal in this case. However, cores were usually polycrystalline, suggesting that the ZnSe crystal grew from several nucleation points inside the apoferritin cavity inner surface (Figure 1). To determine the composition of the cores, EDS analysis of the sample was carried out. The EDS spectra confirmed the presence of zinc and selenium atoms as the elements of the cores (see the Supporting Information). Considering these results together with the TEM observation, the cores shown in Figure 3 are ZnSe NPs. As seen in the figure, more than 90% of apoferritin shells accommodate ZnSe cores. This indicates that our newly designed chemical reaction system works selectively and efficiently.

3.4. XRD Spectra. The structure of the ZnSe NPs synthesized in apoferritin was analyzed using XRD. Figure 4 shows the XRD spectra from ZnSe NP cores. The peaks were broad because of their nanometric size, but the peak

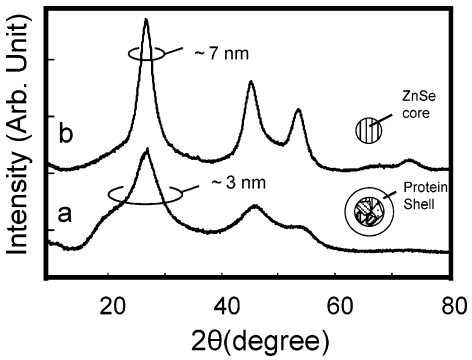

Figure 4. XRD pattern of the ferritin cores as prepared and after heat treatment. Line a shows the XRD pattern from the as-prepared cores. The peaks were vague, but their positions can be determined. The structure of the core was cubic ZnSe. The average crystal size is calculated to be 3 nm using Scherrer's equation. Line b shows the XRD pattern from the cores after 500 °C heat treatment under nitrogen gas. The peaks became sharper, and the average of the crystal size is about 7 nm, which is the same as that of the apoferritin cavity size.

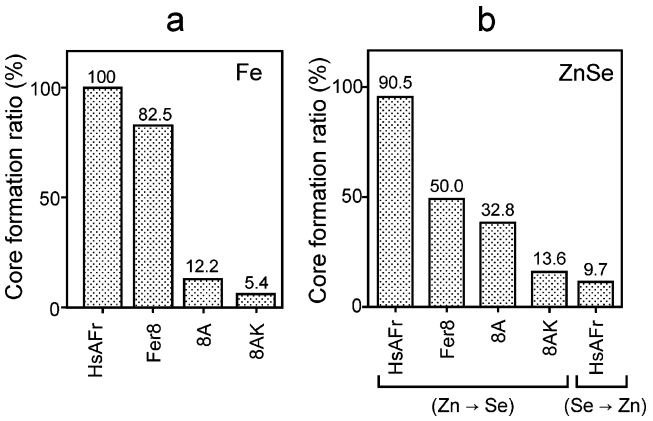

Figure 5. CFRs of Fe and ZnSe NP synthesis in the HsAFr and recombinant apoferritin cavity. (a) The CFR of iron oxide core synthesis. (b) The CFR of ZnSe core synthesis. The CFR was calculated using TEM images stained by aurothioglucose. In the case of ZnSe synthesis (b), Zn → Se indicates that zinc ions were incubated with apoferritin in the optimized synthesis condition and then selenium ions were added last. Se → Zn indicates the reverse addition sequence of zinc and selenium ions to the synthesis mixture.

position can be elucidated. Because the elements of the core were already determined as zinc and selenium atoms, the set of peak positions confirmed that the core structure was ZnSe cubic crystal. The average size of a single ZnSe crystal was calculated from the width of the peak,[18] and the average crystal size synthesized was about 3 nm (Figure 4a). This indicated that the ZnSe NPs cores were not single crystals but polycrystals. To make the core single crystal, we heat-treated the cores under nitrogen gas, avoiding oxidization of the cores. The XRD peaks became sharper after 500 °C heat treatment for 1 h. The spectra show a set of diffraction peaks from the ZnSe cubic crystal, and the average size calculated was around 7 nm (Figure 4b). This is the same size as that of the apoferritin cavity. This result indicated that the polycrystalline ZnSe NP cores could be made into single-crystal NPs by heat treatment. There was no sintering effect. The reason the ZnSe NPs did not sinter is not well understood, but one possibility is that the inactive compounds may make a thin crust at the outermost surface.

The ZnSe−ferritin shows very weak photoluminescence under UV light (Epi-Light FA500; Aisin, Aichi, Japan). It is considered due to the defects in the ZnSe NPs, which may be supported polycrystalline by high-resolution TEM core images (Figure 3).

3.5. Biomineralization Behavior of Positive Ions. The mechanism of ZnSe biomineralization was further studied using recombinant apoferritins. In our theory, the positive zinc ion concentration in the apoferritin cavity plays an important role.

First, we studied how the iron oxide core formation is affected by the recombinant ferritin. Three factors are important for effective iron oxide core formation by HsAFr (CFR is 100% as shown in Figure 5a). (1) The HsAFr consists of the light-chain subunit (L subunit) and the heavy-chain subunit (H subunit). The ferroxidase center in the H subunit oxidizes ferrous iron to ferric iron. (2) HsAFr has negatively charged Asp-131 and Glu-134 amino acid residues (the amino acid is numbered following conventions in preceding literature[15]) lined along the threefold channel surface, which attracts iron ions. (3) The negatively charged Glu-58, Glu-61, and Glu-64 amino acid residues on the inner cavity surface work as nucleation sites, which are highly conserved in mammalian ferritins.

Corresponding to these factors, three types of recombinant apoferritins were constructed: (1) Fer8, the recombinant apoferritins that are composed of only L subunits (no ferroxidase center) and lack the first eight amino acid residues from the N terminal; (2) 8A, the recombinant apoferritin derived from Fer8 in which the Asp-131 and Glu-134 amino acids of the threefold channel were genetically replaced by neutral alanine amino acid residues; (3) 8AK, the recombinant apoferritin derived from 8A, which has the Glu-58, Glu-61, and Glu-64 replaced by the positively charged lysine.

Figure 5a shows the CFR of iron oxide biomineralization by HsAFr and recombinant apoferritins. The CFR of Fer-8 recombinant apoferritin reached 82.5%, even in the absence of a ferroxidase center. This indicates that the ferroxidase center does not make a large difference in the iron oxide core formation *in vitro* and that the autooxidation by the iron oxide surface is fast enough for the iron oxide core formation. This is consistent with the previous report that the Fe^{2+} oxidation rate of the L-chain apoferritin is higher than that of protein-free control.[19,20]

The CFR of 8A recombinant apoferritin decreased dramatically to 12.2% (Figure 5a). There is experimental evidence that these residues of the threefold channel are involved in the uptake of iron ions.[12] The mutation from the negative amino acid residues to the neutral alanine residues in the threefold channel slows down the rates of iron uptake.[21,22] Takahashi and Kuyucak calculated the electrostatic potential at the threefold channel and showed that 8A

(18) Bandaranayake, R. J.; Wen, G. W.; Lin, J. Y.; Jiang, H. X.; Sorensen, C. M. *Appl. Phys. Lett.* **1995**, *67*, 831.

(19) Levi, S.; Luzzago, A.; Cesareni, G.; Cozzi, A.; Franceschinelli, F.; Albertini, A.; Arosio, P. *J. Biol. Chem.* **1988**, *263*, 18086.

(20) Levi, S.; Salfeld, J.; Franceschinelli, F.; Cozzi, A.; Dorner, M. H.; Arosio, P. *Biochemistry* **1989**, *28*, 5179.

has the 4 kT barrier instead of the −46 kT energy well for the Fe^{2+} ion in the case of Fer8 by using the electrostatic calculation methods.[13] Our experimental result of 8A is consistent with these references.

The CFR of 8AK recombinant apoferritin for iron oxide NPs further decreased to 5.4%, suggesting that positively charged iron ions cannot go into the positively charged cavity. These results indicate that not only the negatively charged amino acids of the threefold channel but also three negatively charged amino residues on the inner cavity surface play an important role for the iron oxide NP formation in the apoferritin inner cavity. It is likely that the positive ions are trapped at the threefold channel and then migrate into the apoferritin cavity to make the inorganic cores.

3.6. Elucidation of the Mechanism of ZnSe Biomineralization by the Newly Designed Chemical Reaction System. We investigated the biomineralization of ZnSe using the three recombinant apoferritins and the protocol optimized above.

First, we prepared a Zn^{2+}−apoferritin precursor to study whether Zn^{2+} ions bind to the specific sites in the apoferritin cavity. When 10 mM selenourea was added to the purified Zn^{2+}−apoferritin precursor, about 10% of the apoferritins had thin ZnSe cores. This result indicated that the Zn^{2+} ion occasionally remained in some of the apoferritin cavities. We measured the zinc concentration in the Zn^{2+}−apoferritin precursor by ICP-MASS. A total of 10% of the Zn^{2+}−apoferritin precursors had about 40 zinc ions in the inner cavity. This value is more than that of Watt et al. reported,[26] and there are apoferritins with or without ZnSe cores. These results strongly suggest that there are no irreversible binding specific sites for Zn^{2+} ions in the apoferritin cavity and also indicate that there is equilibrium of Zn^{2+} ions out/in of apoferritin.

We studied the effect of the ferrooxidase center, positively charged threefold channel, and nucleation site of apoferritin on ZnSe biomineralization by using HsAFr and three types of recombinant apoferritins. The CFR of HsAFr for ZnSe was as high as 90.5% (Figure 5b). Different from the iron oxide core case, the CFR of Fer8 decreased to 50.0%. The major difference between HsAFr and Fer8 is the H subunit; Fer8 does not have the H subunit. It has been suggested that the H subunit has an alternative pathway through which iron ions reach the ferroxidase center from outside.[23] It is also suggested that the ferrous ion bound at the ferroxidase center is released into the cavity. In this context, there are reports that zinc ions bind at or near the ferroxidase center in a fashion similar to that of iron ions.[21,24−26] Therefore, the decrease of the Fer8 CFR may be caused by the absence of an H subunit that functions to convey zinc ions from outside into the cavity via the ferroxidase center. This is not conclusively proven, but it is very likely that the ferroxidase center has some relationship with the ZnSe core formation.

The ZnSe CFR of 8A decreased slightly from that of Fer8. This suggests that aspartic and glutamic acid residues of the threefold channel have something to do with the zinc ion uptake. It is also reported that zinc ions bind the threefold channel of HSFr.[21] Then, it is deduced that these negatively charged residues of the threefold channel attract zinc ions to the narrow pathway and the trapped zinc ions are released to the apoferritin cavity in a manner analogous to that of the iron ion case.

The ZnSe CFR of 8AK further dropped to 13.6% (Figure 5b). This is because the positively charged zinc ion hardly penetrates into the apoferritin cavity against the electrostatic energy barrier that is generated by 72 positively charged lysine residues in the 8AK cavity. This result indicates that the electrostatic potential in the apoferritin cavity should be lower than that for the outside cavity for the effective ZnSe biomineralization.

In our new chemical reaction system, the concentration of positive zinc ions in the cavity is the first necessary event and the entrance of the selenium ion should be followed. Therefore, it is anticipated that the reverse addition sequence of zinc and selenium ions should disturb the ZnSe NPs synthesis. We prepared the reaction mixture including 0.3 mg/mL HsAFr, 40 mM ammonium acetate, 7.5 mM ammonia water, and 10 mM selenourea. Zinc acetate (1 mM) was added into this solution. This reverse procedure made the CFR of HsAFr drop dramatically from 90.5% to 9.7% (Figure 5b).

This experimental result can be explained as follows. In the case of the selenium ion addition into the reaction mixture with zinc ions, zinc ions are attracted to the threefold channel and concentrated in the apoferritin cavity. The negative electrostatic potential in the apoferritin cavity was compensated for by the introduced zinc ions. This electrostatic compensation makes it feasible for negatively charged selenium ions to enter the cavity, overcoming the spatial hurdle at the threefold channels. Once the selenium ion reaches the cavity, it reacts quickly with highly concentrated zinc ions in the cavity and forms the ZnSe nucleus, which itself works as a catalyst for ZnSe crystallization. This high zinc ion concentration causes a 20 000 times faster chemical reaction (this is calculated from the cavity size) compared to the bulk solution, where stable tetraaminezinc ion slows down the chemical reaction. In contrast, in the case of zinc ion addition into the reaction mixture with selenium ions, selenium ions are mostly in the bulk solution and very rarely in the apoferritin cavity, because of the negative electrostatic potential in the apoferritin cavity. Zinc ion addition starts ZnSe formation in the bulk solution. There now exists no condition such that ZnSe core formation in the apoferritin cavity can proceed 20 000 times faster than that in the bulk

(21) Treffry, A.; Bauminger, E. R.; Hechel, D.; Hodson, N. W.; Nowik, I.; Yewdall, S. J.; Harrison, P. M. *Biochem. J.* **1993**, *296*, 721.
(22) Levi, S.; Santambrogio, P.; Corsi, B.; Cozzi, A.; Arosio, P. *Biochem. J.* **1996**, *317*, 467.
(23) Lawson, D. M.; Artymiuk, P. J.; Yewdall, S. J.; Smith, J. M. A.; Livingstone, J. C.; Treffry, A.; Luzzago, A.; Levi, S.; Arosio, P.; Cesareni, G.; Thomas, C. D.; Shaw, W. V.; Harrison, P. M. *Nature* **1991**, *349*, 541.
(24) Baaghil, S.; Lewin, A.; Moore, G. R.; Brun, N. E. L. *Biochemistry* **2003**, *42*, 14047.
(25) Treffry, A.; Harrison, P. M. *J. Inorg. Biochem.* **1984**, *21*, 9.
(26) Pead, S.; Durrant, E.; Webb, B.; Larsen, C.; Heaton, D.; Johnson, J.; Watt, G. D. *J. Inorg. Chem.* **1995**, *59*, 15.
(27) Tsukamoto, R.; Iwahori, K.; Muraoka, M.; Yamashita, I. *Bull. Chem. Soc. Jpn.*, in press.

solution. Therefore, ZnSe is synthesized mainly as bulk precipitation, and little core formation inside the cavity was observed.

Taking all of the information obtained into consideration, it is likely that the ZnSe core formation has occurred by two steps. At first, zinc ions are attracted by the negatively charged threefold channel and go through the threefold channels into the apoferritin cavity. Then, zinc ions are attracted by the negatively charged nucleation sites on the cavity surface and are concentrated. Second, the selenium ions go through the threefold channels and reach the zinc ions at the inner surface of the apoferritin cavity to make nuclei for the ZnSe core. These nuclei work as autocatalysts and make the ZnSe cores.

4. Conclusion

ZnSe NPs were successfully synthesized in the apoferritin cavity by designing a chemical reaction system that is composed of a slow chemical reaction system and a two-step synthesis protocol. The slow chemical reaction makes use of a stable tetraaminezinc ion and an unstable selenourea. The two-step synthesis is composed of a first step, incubation of teraaminezinc with an apoferritin molecule, and a second step, addition of selenourea. The best condition for the slow chemical reaction system of ZnSe NPs was determined, and ZnSe NPs were formed in the apoferritin cavity in a spatially selective manner. The CFR is more than 90%, and little bulk precipitation was observed. The characterization of prepared ZnSe NPs by EDS analysis and XRD revealed that the as-prepared ZnSe cores were composed of several ZnSe cubic crystals and they became single crystals by 500 °C heat treatment for 1 h under nitrogen gas. The ZnSe biomineralization experiments using recombinant apoferritin indicate that the glutamic and aspartic acid residues of the threefold channel and apoferritin inner surface play a very important role for ZnSe NP formation in the apoferritin cavity and support our theory. This is the first successful synthesis of a ZnSe compound semiconductor using a biotemplate. This biological pathway will open up a new approach for the development of NP synthesis.

Acknowledgment. We thank H. Furusho for the high-resolution TEM observation and EDS measurement and Dr. M. Okuda for the measurement of ICP-MASS and valuable discussions.

Supporting Information Available: EDS spectrum of ZnSe−ferritin. This material is available free of charge via the Internet at http://pubs.acs.org.

IC0502426